Macromolecules **1998,** *31,* 479−483

Charge Transport and Spin Dynamics of Chemically Synthesized Polypyrrole Soluble in Organic Solvents

J. Joo,* J. K. Lee, J. K. Hong, and J. S. Baeck

Department of Physics, Korea University, Seoul 136-701, Korea

W. P. Lee

Department of Physics, The Ohio State University, Columbus, Ohio 43210

A. J. Epstein

Department of Physics and Department of Chemistry, The Ohio State University, Columbus, Ohio 43210-1106

K. S. Jang, J. S. Suh, and E. J. Oh

Department of Chemistry, Myongji University, Yong-In 449-728, Korea

Received April 15, 1997; Revised Manuscript Received September 15, 1997[⊗]

ABSTRACT: The results of the temperature dependence of dc conductivity, microwave dielectric constant, X-ray diffraction, EPR, and NMR experiments are reported for chemically synthesized polypyrrole films soluble in organic solvents. The temperature dependence of dc conductivity of these systems follows the three-dimensional variable range hopping model. The slope of the temperature dependence of dc conductivity varies with dopants and solvents used. Room temperature dc conductivities are in the range of ∼0.2−0.01 S/cm, and the localization lengths are estimated as ≤10 Å, which indicates a relatively strong localization of charge. The results of microwave dielectric constant experiments support the strong localization behavior. The X-ray diffraction studies show that soluble polypyrroles are amorphous. From electron paramagnetic resonance experiments, the density of states of polypyrrole doped with naphthalenesulfonic acid in *m*-cresol solvent is estimated as ∼0.107 states/(eV ring). We obtain the result that the system achieves a more highly conducting state as the polarity of the solvent used increases.

Introduction

Pristine (undoped) polypyrrole (PPy) is a π-conjugated polymer, which is formed by the overlap of carbon p_z orbitals and alternating carbon and carbon bond length.[1,2] Polyacetylene, poly (*p*-phenylenevinylene), and polythiophene are also conjugate systems. The interchange of single and double bonds in PPy leads to a different energy state, which indicates that PPy has a nondegenerate ground state, while polyacetylene has a doubly degenerate insulating ground state.[2,3] Through the doping process, the conductivity of PPy is changed from insulating ($\sigma_{dc} \leq 10^{-7}$ S/cm) to metallic ($\sigma_{dc} \geq 10^2$ S/cm).[2] The presence of polarons or bipolarons at low doping and of a polaron lattice or partially filled energy band for highly doping have been proposed for the variation of conductivity of nondegenerate systems including PPy.[2,4−7]

The charge transport of PPy has been studied for electrochemically synthesized materials.[6,8−12] Pfluger and Street reported the existence of interchain links or branches (about 30%) through the 2,3 positions in a pyrrole ring based upon an X-ray photoelectron spectroscopy (XPS) study of the electrochemically synthesized PPy samples,while most of pyrrole units are linked at the 2,5 positions to form straight chains.[13,14] Though the 2,3 coupling mode might increase the mechanical strength of the system, it reduces the solubility of PPy in organic solvents. Recent progress in chemical synthesis using various dopants and organic solvents has contributed to the development of soluble PPy.[15,16] Relatively large size dopants such as dodecylbenzenesulfonic acid (DBSA) or naphthalenesulfonic acid (NSA) are used to reduce the interchain interaction of polypyrrole chains resulting in solubility in various organic solvents. For chemically synthesized soluble polyaniline (PAN) materials, the charge transport properties vary with dopants and solvents used.[17−19] The interchain interaction, the conformational change of polymer chains, and the hydrogen bonds between polymer backbone, dopant, and solvent are important for the conductivity and its temperature dependence in the PAN system.

In this report, we investigate the effects of the dopant and the solvent on charge transport and spin dynamics in soluble PPy systems. The results of the temperature-dependent dc conductivity [$\sigma_{dc}(T)$] are presented for polypyrrole samples doped with DBSA and NSA, which are soluble in dimethyl sulfoxide (DMSO), *N*-methyl-2-pyrrolidinone (NMP), *m*-cresol, chloroform ($CHCl_3$), and dichloromethane (CH_2Cl_2) solvents. The temperature dependencies of σ_{dc} are fit by the three-dimensional variable range hopping model, $\sigma_{dc}(T) \propto \exp(-(T_0/T)^{1/4})$. The systems becomes more highly conducting with increasing polarity of the solvent used. We conclude that the interchain interaction and the interdopant Coulomb repulsion depend upon the polarity of the solvent and that they are important for the charge transport properties of the system. The density of states obtained from electron paramagnetic resonance (EPR) experiments and the spin−lattice relaxation time from

---

* To whom correspondence should be addressed. E-mail: jjoo@kuccnx.korea.ac.kr. FAX: 82-2-927-3292.

[⊗] Abstract published in *Advance ACS Abstracts,* December 15, 1997.

S0024-9297(97)00508-1 CCC: $15.00

^{1}H NMR experiments also are presented in this paper.

Experimental Section

Distilled pyrrole monomer (0.23 mol) and dopant (0.08 mol of DBSA or NSA) were dissolved in distilled water under magnetic stirring at 5 °C. For an oxidant, 0.05 mol of $(NH_4)_2S_2O_8$ was dissolved in distilled water at the same temperature. The solution containing oxidant was poured into the solution of pyrrole and dopant under magnetic stirring. Polymerization was carried out for 30 h at 5 °C in air. PPy powder was filtered and washed with methanol, and dried under dynamic vacuum for 48 h. Free standing films were cast from homogeneous solutions of doped polypyrrole dissolved in various solvents such as DMSO, NMP, *m*-cresol, $CHCl_3$, or CH_2Cl_2 onto glass substrates. The films were dried on a hot plate in air for 10 h at 60– 80 °C.

A four-probe method was used for measuring dc conductivity in order to eliminate contact resistance. The measured temperature range for σ_{dc} was from 300 to 10 K using a Janis closed-cycle refrigerator system (CCS-100). Four thin gold wires (0.05-mm thick and 99% pure gold) were attached in parallel on the sample surface by conducting graphite paint (Acheson Electrodag 502) for better electrical contact. The EPR spectra for magnetic susceptibility (χ) were obtained using a Bruker ESP300 spectrometer (X-band). The measured temperature range for the EPR experiments was from 300 to 100 K. The susceptibility of the system was estimated from the EPR integrated intensities calibrated against a LiF crystal standard. For ^{1}H NMR experiments, a Bruker MSL 200 FT-NMR was used with the magnetic field fixed at 4.7 T. The microwave cavity perturbation (MCP) method[20,21] was used to measure the temperature dependence of the dielectric constant. The resonance frequency of the MCP system was 6.5 GHz.

Results and Discussion

The temperature dependencies of the dc conductivity [$\sigma_{dc}(T)$] for soluble polypyrrole (PPy) using NSA and DBSA as the dopants prepared with various organic solvents such as NMP, *m*-cresol, and $CHCl_3$ are presented in Figure 1. The three-dimensional (3D) variable range hopping (VRH) model, which is described in ref 22, provides the best fitting for $\sigma_{dc}(T)$:

$$\sigma_{dc}(T) = \sigma_0 T^{-1/2} \exp[-(T_0/T)^{1/4}] \qquad (1)$$

Here, T_0 is $16/[k_B N(E_F) L^3]$, where k_B is the Boltzmann constant, $N(E_F)$ is the density of states at the Fermi level and L is the localization length.[22]

The density of states, $N(E_F)$, was obtained from the measurement of susceptibility (χ) through EPR experiments. Figure 2 presents χT of PPy–NSA (*m*-cresol) and PPy–DBSA (*m*-cresol) samples as a function of temperature. Considering $\chi = \chi^{Pauli} + \chi^{Curie}$ where χ^{Pauli} is independent of temperature and $\chi^{Curie} \propto 1/T$, the slope of the straight line of T provides the χ^{Pauli}.[12,18] Using the relation $\chi^{Pauli} = 2\mu_B{}^2\, N(E_F)$ where μ_B is the Bohr magneton, and the density of states, $N(E_F)$, is estimated as ~0.107 and ~0.072 st./(eV ring) for PPy–NSA (*m*-cresol) and PPy–DBSA (*m*-cresol) materials, respectively. We assumed that $N(E_F)$ is independent of the solvent used to estimate the localization length.

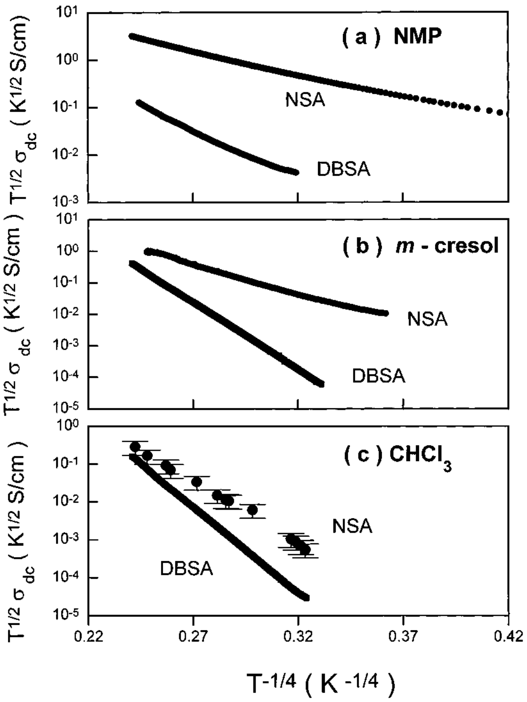

Figure 1. Comparison of the temperature dependence of dc conductivity for soluble PPy–NSA and PPy–DBSA samples processed from the same solvent: (a) NMP; (b) *m*-cresol; (c) $CHCl_3$.

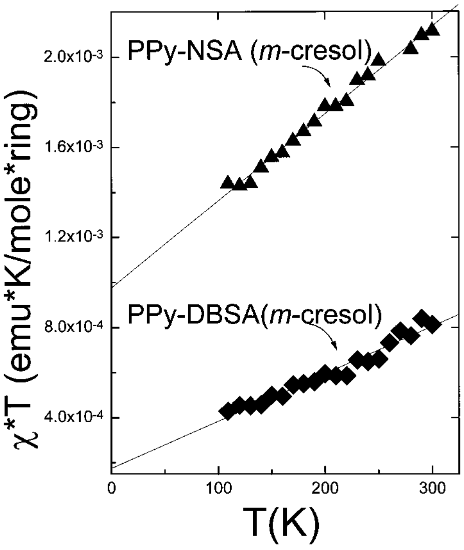

Figure 2. χT vs T obtained from the EPR experiments for PPy–NSA (*m*-resol) and PPy–DBSA (*m*-cresol) samples.

The dc conductivities of PPy–NSA samples processed from NMP, *m*-cresol, and $CHCl_3$ solvents are higher and their temperature dependencies are weaker than those of the corresponding PPy–DBSA samples, Figure 1. The DBSA dopant is larger than the NSA dopant, Figure 3, leading to weaker interchain interaction (a relatively large interchain distance for hopping) and the lower conductivity of PPy–DBSA materials. Figure 4 compares the $\sigma_{dc}(T)$ of soluble PPy prepared in different solvents with the same dopant. The room temperature dc conductivities are in the range of ~0.2–0.01 S/cm. PPy–NSA (DMSO) is the highest conducting material, while PPy–DBSA prepared with $CHCl_3$ solvent is the lowest conducting one. For the PPy–NSA (DMSO) sample, σ_{dc} at room temperature is ~0.2 S/cm and the localization length (L) is estimated as ~10 Å by using eq 1. As the temperature decreases, σ_{dc} decreases, indicating the charge localization in the system. The slope (T_0) of $\sigma_{dc}(T)$ sensitively depends on the polarity of the solvents used. The temperature dependencies of σ_{dc} of PPy–NSA (*m*-cresol) and PPy–NSA ($CHCl_3$) samples are stronger than those of PPy–NSA (DMSO) and PPy–NSA (NMP). In Figure 4 (b), σ_{dc} values of PPy–DBSA in *m*-cresol and $CHCl_3$ solvents have strong

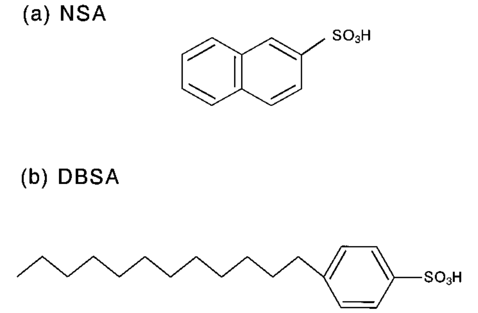

Figure 3. Schematic chemical structure of (a) naphthalenesulfonic acid (NSA) and (b) dodecylbenzenesulfonic acid (DBSA).

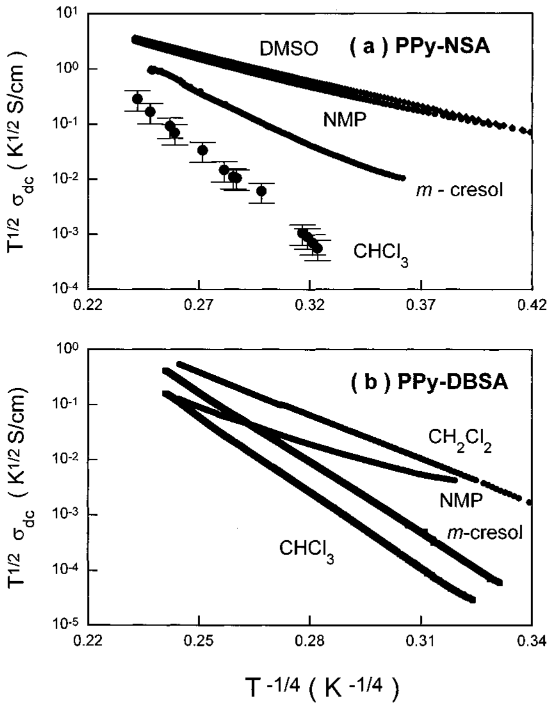

Figure 4. Temperature dependence of dc conductivity of soluble PPy in various solvents doped with (a) NSA and (b) DBSA.

temperature dependencies, and the L is estimated as ≤ 2 Å, which implies a strong localization of the charge. However, T_0's of PPy−DBSA (NMP) and PPy−DBSA (CH_2Cl_2) samples are relatively small ($\sim 4.5 \times 10^6$ K and $\sim 1.3 \times 10^7$ K), and the L's are estimated as $\sim$4 and $\sim$3 Å, respectively. It is noted that the 3D VRH of the system contrasts with the results for electrochemically synthesized PPy samples, which have similar room temperature dc conductivities ($\sim 1 - 10^{-2}$ S/cm), reported by Chauvet *et al.*,[6] but have $\ln \sigma_{dc} \propto T^{-1/2}$.

The results of X-ray diffraction experiments of PPy−NSA samples processed from various solvents are presented in Figure 5. A broad diffraction peak was detected at $2\theta \approx 18°$ for the measured samples, indicating that the systems are strongly disordered. The PPy−NSA (DMSO) sample, which is the highest conducting sample, has a better crystallinity than PPy−NSA (NMP) and PPy−NSA ($CHCl_3$).

Figure 6 shows the dependence of the localization length (L) on the polarity of the solvents and the dopants. As the polarity of the solvents for the same dopant increases [$CHCl_3$ (nonpolar, $\epsilon = 4.86$) < CH_2Cl_2 ($\epsilon = 8.65$) < *m*-cresol ($\epsilon = 12.4$) < NMP ($\epsilon = 32.2$) < DMSO (polar, $\epsilon = 46.5$), where ϵ is the dielectric constant],[23] the temperature dependence of σ_{dc} weakens, and the localization length increases; i.e., it approaches a more highly conducting state for both NSA and DBSA dopants. *In polar solvents such as NMP or DMSO, large size dopants (DBSA and NSA) might be positioned as close as possible to the polymer chains due to screening of interchain and the interdopant coulomb repulsion. This would improve interchain structural correlations, thereby improving interchain charge transport, increasing dc conductivity and reducing the temperature dependence of* σ_{dc}*. However in less polar solvents where screening is negligible, the volume occupied by dopant is expected to be relatively large, thereby inducing the weak interchain interaction.*

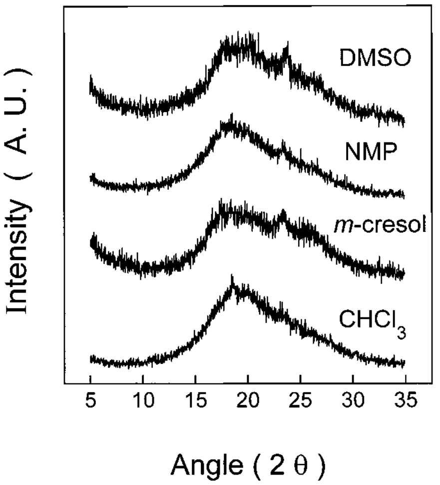

Figure 5. Comparison of X-ray diffraction patterns of PPy−NSA processed from various solvents (DMSO, NMP, *m*-cresol, and $CHCl_3$).

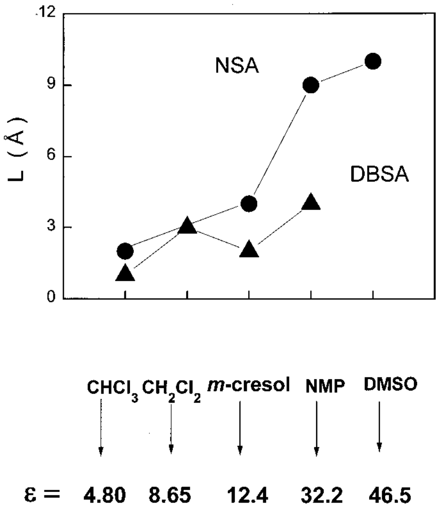

Figure 6. Dependence of localization length (L) of soluble PPy on the nature of dopants and solvents used.

Microwave dielectric constants (ϵ_{mw}) of PPy−DBSA (*m*-cresol) and PPy−DBSA ($CHCl_3$) samples as a function of temperature are compared in Figure 7. The room temperature ϵ_{mw} of both samples is less than 100, indicating a relatively strong localization. The ϵ_{mw} for the PPy−DBSA (*m*-cresol) sample is higher than that of PPy−DBSA ($CHCl_3$) throughout the measured temperature range, which implies that PPy−DBSA (*m*-cresol) is less localized in accord with $\sigma_{dc}(T)$. One can estimate the localization length by using ϵ_{mw} and a metallic box (MB) model.[24,25] From the MB model, the real part of the dielectric constant at a finite frequency

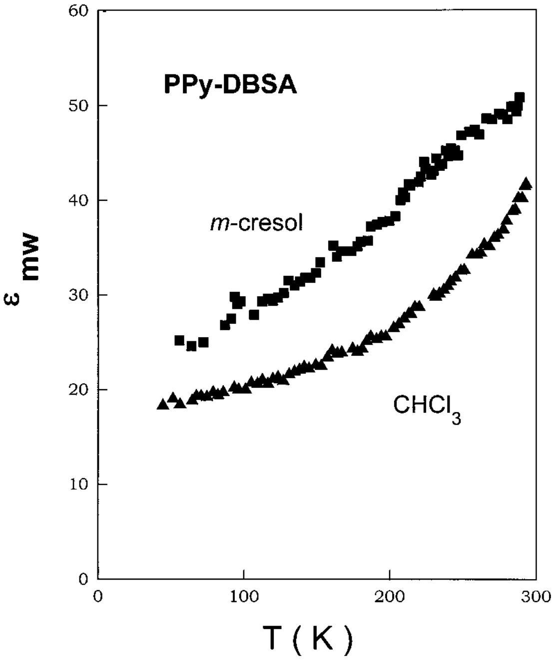

Figure 7. Temperature dependence of microwave dielectric constant ($\epsilon_{\rm mw}$) of PPy–DBSA in *m*-cresol and CHCl$_3$ solvents.

is described as[17,24,26]

$$\epsilon_{\rm mw}(T \to 0) \approx \epsilon_\infty + \frac{2^{9/2}}{\pi^3} e^2 N(E_{\rm F}) L^2 \qquad (2)$$

where $\epsilon_{\rm mw}(T \to 0)$ is the microwave dielectric constant as temperature (T) approaches 0 K, ϵ_∞ the core polarization, and e the electron charge. The localization length of both samples is estimated as $\leq$10 Å, which agrees with the charge being in the strongly localized regime.

The spin–lattice relaxation time (T_1) of the system was determined from the inversion recovery method in ^{1}H NMR experiments.[27] The relation between the proton magnetization and the T_1 can be described as

$$\frac{M_z(\tau)}{M_0} = 1 - 2\exp\left(-\frac{\tau}{T_1}\right) \qquad (3)$$

where $M_z(\tau)$ is the proton magnetization at time τ and M_0 is the total proton magnetization.[27] Figure 8 shows the temperature dependence of T_1 for PPy–DBSA and PPy–NSA samples. With the same dopant, the T_1 values are not sensitive to the solvent used. At room temperature, T_1 for PPy–DBSA (NMP) and PPy–DBSA (CH$_2$Cl$_2$) is 3.3 and 2.8 s, respectively, while T_1 for PPy–NSA samples is less than 2.5 s. The estimated T_1 values of PPy–DBSA samples are larger than those of PPy–NSA throughout the measured temperature range. This implies that the spin–lattice interaction in PPy–NSA materials more easily occurs due to the relatively small size of dopant.[28] The T_1 value decreases with decreasing temperature, which is similar to the trend of $\sigma_{\rm dc}(T)$. Therefore, the interchain interaction and the lattice phonon are important for the value of T_1 and its temperature dependence.

Conclusions

Charge transport properties such as the temperature dependence of dc conductivity and microwave dielectric constant of chemically synthesized soluble polypyrrole samples vary with dopants and solvents used. As the polarity of the solvent increases, the system achieves a more highly conducting state. With the same solvent, the dc conductivity of PPy–NSA systems is higher than that of PPy–DBSA, likely induced by stronger interchain interaction due to the smaller dopant size. The three-dimensional variable range hopping model provides the best fit to the temperature dependence of dc conductivity. Relatively small localization lengths ($L \leq 10$ Å) estimated from $\sigma_{\rm dc}(T)$ and $\epsilon_{\rm mw}$ (T) indicate that the charge motion is in the strongly localized regime. From the EPR experiments, the density of states of these systems are estimated to be 0.107 and 0.072 st./(eV ring) for PPy–NSA (*m*-cresol) and PPy–DBSA (*m*-cresol), respectively. From ^{1}H NMR experiments, the spin–lattice relaxation times (T_1) were obtained. The short T_1 of PPy–NSA compared to that of PPy–DBSA implies that the spin–lattice interaction more easily occurs in the system with the smaller dopant size.

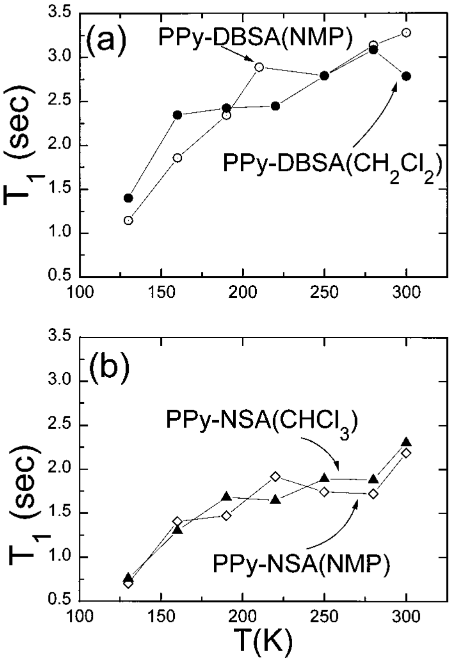

Figure 8. Temperature dependence of spin–lattice relaxation time (T_1) for (a) PPy–DBSA (NMP) and PPy–DBSA (CH$_2$Cl$_2$) and (b) PPy–NSA (CHCl$_3$) and PPy–NSA (NMP) samples.

Acknowledgment. This work was supported in part by Basic Science Research Grant (BSRI-96-2444, BSRI-97-2444) of the Ministry of Education, Korea, Advanced Materials Chemistry Research Center in Korea University (Korea Research Foundation), and Grant NSF-DMR-950873, from the NSF.

References and Notes

(1) Skotheim, T. A., Ed. *Handbook of Conducting Polymers*; Marcel Dekker: New York, 1986.

(2) Kohlman, R. S.; Joo, J.; Epstein, A. J. In *Physical Properties of Polymers Handbook*; Mark, J. E., Ed.; American Institute of Physics: New York, 1996; p 453 and references therein.

(3) Heeger, A. J.; Kivelson, S. A.; Schrieffer, J. R.; Su, W. P. *Rev. Mod. Phys.* **1988**, *60*, 781.

(4) Kaufman, J. H.; Colaneri, N.; Scott, J. C.; Street, G. B. *Phys. Rev. Lett.* **1984**, *53*, 1005.

(5) Bredas, J. L.; Scott, J. C.; Yakushi, K.; Street, G. B. *Phys. Rev. B* **1984**, *30*, 1023.

(6) Chauvet, O.; Paschen, S.; Forro, L.; Zuppiroli, L.; Bujard, P.; Kai, K.; Wernet, W. *Synth. Met.* **1994**, *63*, 115.

(7) Pluger, P.; Krounbi, M.; Street, G. B.; Weiser, G. *J. Chem. Phys.* **1983**, *78*, 3212.

(8) Yoon, C. O.; Reghu, M.; Moses, D.; Heeger, A. J. *Phys. Rev. B* **1994**, *49*, 10851.

(9) Zuppiroli, L.; Bussac, M. N.; Paschen, S,; Chauvet, O.; Forro, L. *Phys. Rev. B* **1994**, *50*, 5196.

(10) Sixou, B.; Mermilliod, N.; Travers. J. P. *Phys. Rev. B* **1996**, *53*, 4509.

(11) Ishiguro, T.; Kaneko, H.; Nogami, Y.; Ishimoto, H.; Nishiyama, H.; Tsukamoto, J.; Takahashi, A.; Yamaura, M.; Sato, K. *Phys. Rev. Lett.* **1992**, *69*, 660.

(12) Kohlman, R. S.; Joo, J.; Wang, Y. Z.; Pouget, J. P.; Kaneko, H.; Ishiguro, T.; Epstein, A. J.; *Phys. Rev. Lett.* **1995**, *74*, 773.

(13) Pfluger, P.; Street, G. B. *J. Chem. Phys.* **1984**, *80*, 544.

(14) Kanatzidis, M. G. *Chem. Eng. News* **1990**, Dec 3, 36.

(15) Lee, J. Y.; Kim, D. Y.; Kim, C. Y. *Synth. Met.* **1995**, *74*, 103. Kim, D. Y.; Lee, J. Y.; Kim, C. Y.; Kang, E. T.; Tan, K. L. *Synth. Met.* **1995**, *72*, 243.

(16) Oh, E. J.; *et al.* To be submitted for publication.

(17) Joo, J.; Oblakowski, Z.; Du, G.; Pouget, J. P.; Oh, E. J.; Wiesinger, J. M.; Min, Y.; MacDiamid, A. G.; Epstein, A. J. *Phys. Rev. B* **1994**, *49*, 2977.

(18) Epstein, A. J.; Joo, J.; Kohlman, R. S.; Du, G.; MacDiarmid, A. G.; Oh, E. J.; Min, Y.; Tsukamoto, J.; Kaneko, H.; Pouget, J. P. *Synth. Met.* **1994**, *65*, 149.

(19) Joo, J.; Song, H. G.; Chung, Y. C.; Baeck, J. S.; Jeong, S. K.; Suh, J. S.; Oh, E. J. *J. Korean Phys. Soc.* **1997**, *40*, 230.

(20) Buravov, L.; Shchegolev, I. F. *Prib. Tekh. Eksp.* **1971**, *2*, 171 [*Instrum. Exp. Tech. (Engl. Transl.)* **1971**, *14*, 528].

(21) Wang, Z. H.; Scherr, E. M.; MacDiarmid, A. G.; Epstein, A. J. *Phys. Rev. B* **1992**, *45*, 4190.

(22) Mott, N. F.; Davis, E. *Electronic Processes in Non-Crystalline Materials*; Clarendon Press: Oxford, England, 1979.

(23) Riddick, J. A.; Bunger, W. B.; Sakano, T. K. *Techniques of Chemistry*; *Organic Solvents-Physical Properties and Methods of Purification*, 4th ed.; Wiley: New York, 1986, Vol. 2.

(24) Cini, M.; Ascarell, P. *J. Phys. F* **1974**, *4*, 1998.

(25) Rice, M. J.; Bernasconi, J. *J. Phys. F* **1972**, *2*, 905.

(26) Wang, Y. Z.; Joo, J.; Hsu, C. -H.; Pouget, J. P.; Epstein, A. J. *Macromolecules* **1994**, *27*, 5871.

(27) Fukushima, E.; Roeder, B. W. *Experimental Pulse NMR*; Addison-Wesley Publishing Co.: London, 1981.

(28) In two-dimensions, the size of DBSA and NSA dopants is estimated as ~ 22 × 2.5 Å^2 and ~ 7.6 × 3.7 Å^2, respectively.

MA970508V